Single-Step High-Yield Radiosynthesis and Evaluation of a Sensitive ^{18}F-Labeled Ligand for Imaging Brain Peripheral Benzodiazepine Receptors with PET

Emmanuelle Briard, Sami S. Zoghbi, Fabrice G. Siméon, Masao Imaizumi, Jonathan P. Gourley, H. Umesha Shetty, Shuiyu Lu, Masahiro Fujita, Robert B. Innis, and Victor W. Pike*

Molecular Imaging Branch, National Institute of Mental Health, National Institutes of Health, Building 10, Room B3 C346A, 10 Center Drive, Bethesda, Maryland 20892

Received September 19, 2008

Elevated levels of peripheral benzodiazepine receptors (PBR) are associated with activated microglia in their response to inflammation. Hence, PBR imaging in vivo is valuable for investigating brain inflammatory conditions. Sensitive, easily prepared, and readily available radioligands for imaging with positron emission tomography (PET) are desirable for this purpose. We describe a new ^{18}F-labeled PBR radioligand, namely [^{18}F]*N*-fluoroacetyl-*N*-(2,5-dimethoxybenzyl)-2-phenoxyaniline ([^{18}F]**9**). [^{18}F]**9** was produced easily through a single and highly efficient step, the reaction of [^{18}F]fluoride ion with the corresponding bromo precursor, **8**. Ligand **9** exhibited high affinity for PBR in vitro. PET showed that [^{18}F]**9** was avidly taken into monkey brain and gave a high ratio of PBR-specific to nonspecific binding. [^{18}F]**9** was devoid of defluorination in rat and monkey and gave predominantly polar radiometabolite(s). In rat, a low level radiometabolite of intermediate lipophilicity was identified as [^{18}F]2-fluoro-*N*-(2-phenoxyphenyl)acetamide ([^{18}F]**11**). [^{18}F]**9** is a promising radioligand for future imaging of PBR in living human brain.

Introduction

Peripheral benzodiazepine receptors (PBR[a]) are located on heteropolymeric 18 kDa proteins[1] and their complexes and have a uniquely strong avidity for certain benzodiazepines (e.g., 4′-chlorodiazepam).[2] PBR were initially discovered as diazepam binding sites in kidney[3] and are now known to be widespread[4] in peripheral organs including not only kidney but also lung, heart, and endocrine glands. Relatively low levels of PBR are also found in normal brain.[5] The structure and functions of PBR are wholly distinct from those of the well-known brain benzodiazepine receptors that are acted upon by endogenous GABA or by well-known therapeutic benzodiazepines such as diazepam. Consequently, it has recently been suggested to rename PBR as the "translocator protein (18 kDa)" or TP-18.[6] PBR are primarily located at outer mitochondrial membranes[1] within transmembrane channels[7] that have many putative functions, including cholesterol transport,[8] porphyrin transport,[9] immunomodulation,[10] cell proliferation,[11] and apoptosis.[12] PBR are present in activated microglia[13] and to a lesser extent in astrocytes,[14] and hence PBR concentrations are found to be elevated in regions of brain inflammation arising from neurodegenerative disorders (e.g., multiple sclerosis, Alzheimer's disease) or brain trauma (e.g., stroke).[15−17] Imaging of PBR in vivo is therefore recognized as a means to detect and investigate neuroinflammation.[18] The radioligand [^{11}C]PK 11195[19] ([*N*-*methyl*-^{11}C]1-(2-chlorophenyl)-*N*-methyl-*N*-(1-methylpropyl)-3-isoquinoline carboxamide), preferably as its *R*-enantiomer,[20] has long been used with positron emission tomography (PET) for such investigations[21] but is widely recognized to lack both sensitivity and amenability to quantitation of in vivo binding parameters.[22]

Chart 1. Ligands and PET Radioligands Based on the Aryloxyanilide **1**[a]

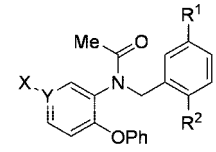

1 X-Y = F*-C, R^1 = OMe, R^2 = OMe*
2 X-Y = H-C, R^1 = H, R^2 = CO_2Me*
3 X-Y = N, R^1 = H, R^2 = OMe*
4 X-Y = F-C, R^1 = OMe, R^2 = OCH_2F*
5 X-Y = F-C, R^1 = OMe, R^2 = OCH_2CH_2F*
6 X-Y = N, R^1 = H, R^2 = OCH_2CH_2F*

[a] An asterisk indicates a site in which the ligand has been labeled with either carbon-11 or fluorine-18.

Potent ligands for PBR are known from many different structural classes[23] and many have been explored as potential PET radioligands.[22] Aryloxyanilides, related to the high-affinity and selective PBR ligand, **1** (DAA1106),[24] have become an especially abundant source of candidate radioligands (Chart 1). PBR radioligands in this class, which have a carbon-11 label and that are more sensitive and effective than [^{11}C]PK 11195, are now known, including [^{11}C]**1**.[25] One of the most promising is [^{11}C]**3** ([^{11}C]PBR28).[26−29] Nevertheless, the use of such radioligands is necessarily restricted to imaging facilities either at or very close to their site of production because of the short half-life of carbon-11 ($t_{1/2}$ = 20.4 min; β^+ = 99.8%).

Alternative labeling with fluorine-18 ($t_{1/2}$ = 109.7 min; β^+ = 97%) opens up several advantages over labeling with carbon-11. First, high (multi-Ci) activities of fluorine-18, as [^{18}F]fluoride ion, can be produced from moderate energy cyclotrons by the ^{18}O(p,n)^{18}F reaction on [^{18}O]water.[30] Second, the longer half-life allows transport over considerable distances to remote PET

* To whom correspondence should be addressed. Phone: 301 594 5986. Fax: 301 480 5112. E-mail: pikev@mail.nih.gov.

[a] Abbreviations: CA, carrier-added; D, dopaminergic; DAT, dopamine transporter; GABA, γ-aminobutyric acid; H, histaminergic; HPLC, high-performance liquid chromatography; K 2.2.2, 4,7,13,18-tetraoxa-1,10-diazabicyclo[8.8.8]hexacosane; NCA, no-carrier-added; PET, positron emission tomography; PBR, peripheral benzodiazepine receptors; RCY, decay-corrected radiochemical yield; MR, magnetic resonance; NET, noradrenaline transporter; rt, room temperature; SERT, serotonin transporter; SR, specific radioactivity; SUV, standardized uptake value; TAC, time-activity curve; VOI, volume of interest; 5-HT, serotonin.

10.1021/jm8011855
Published on Web 01/02/2009

Scheme 1. Synthesis of **9** and [^{18}F]**9**[a]

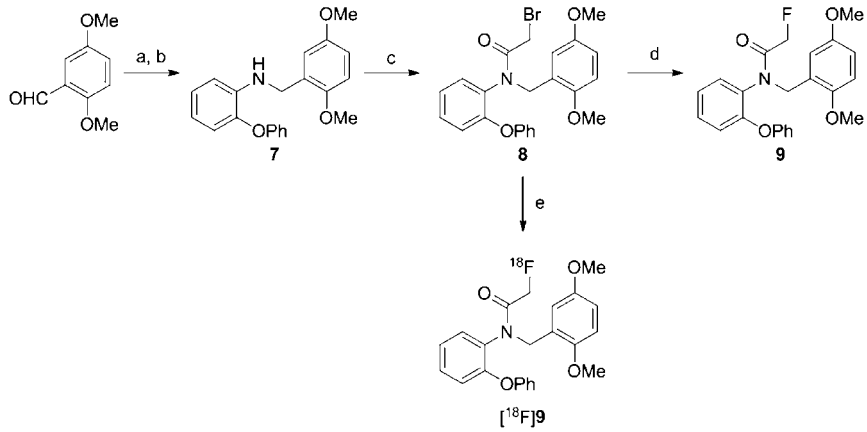

[a] Reaction conditions and yields. (a) 2-phenoxyaniline, MeOH, rt, 24 h; (b) $NaBH_4$, rt, 1 h; 75% for steps a plus b overall; (c) bromoacetyl bromide, CH_2Cl_2, Et_3N, 0 °C, 1 h; 73%; (d) KF, di(ethylene glycol), 150 °C, 4 h; 95%; (e) [^{18}F]fluoride ion, MeCN-trace water, 18-crown-6, $KHCO_3$, 110 °C, 10 min; RCY 97%, or [^{18}F]fluoride ion; MeCN, K 2.2.2, K_2CO_3, 100 °C, 20 min; isolated and formulated RCY, 12.2%.

centers and also allows longer and more accurate imaging sessions. Finally, fluorine-18 emits a low-energy positron during decay, and this permits the high spatial resolution of modern PET cameras (~2 mm) to be fully utilized. So far, only two ^{18}F-labeled ligands, [^{18}F]**4** ([^{18}F]FMDAA1106) and [^{18}F]**5** ([^{18}F]FEDAA1106) (Chart 1), have been developed from the aryloxyanilide class[31,32] and evaluated with PET imaging in animal or human subjects.[33] However, each of their preferred methods of radiosynthesis requires two steps and is overall inefficient. The single-step labeling of **1** with fluorine-18 in high radiochemical yield has recently been described.[34] No evaluation of this radioligand in vivo has yet been reported, although the ^{11}C-labeled version has appeared promising in mouse[25] and monkey.[35] Recently, another ^{18}F-labeled aryloxyanilide radioligand for PBR, namely [^{18}F]**6** ([^{18}F]-FEPPA), was labeled in a single-step, but its preliminary evaluation in rats was incomplete with regard to characterizing its behavior and therefore its potential for PBR imaging in higher species.[36] Only a few other ^{18}F-labeled PBR ligands are known. One is a close analogue of [^{11}C]PK 11195, namely [^{18}F]1-(2-fluoro-5-nitrophenyl)-*N*-methyl-*N*-(1-methylpropyl)-3-isoquinoline carboxamide ([^{18}F]PK 14105),[37] which was shown to be a marker of brain ischemic lesions in rat,[38] but which has not been progressed to human evaluation. Another is a recently reported[39] high-affinity [^{18}F]fluoropropyl analogue of iodo-PK 11195, whose imaging properties have not yet been described. Recently, candidate ^{18}F-labeled ligands from other structural classes (imidazo[1,2-*a*]pyridines and pyrazolo[1,5-*a*]pyrimidines) have been synthesized and evaluated in rats. However, even the most promising of these radioligands suffers from extensive metabolism and defluorination.[40] Therefore, there is still a clear need for an easily prepared and effective ^{18}F-labeled ligand for brain PBR imaging.

Here we report the radiosynthesis of a new ^{18}F-labeled PBR ligand, [^{18}F]*N*-fluoroacetyl-*N*-(2,5-dimethoxybenzyl)-2-phenoxyaniline ([^{18}F]**9**; Scheme 1) in a single efficient radiosynthetic step that was easily incorporated into automated radiosynthesis devices. Our evaluation of [^{18}F]**9** in monkey and rat showed that this radioligand is sensitive for imaging PBR with PET and has high promise for imaging of PBR in living human brain.

Results

Chemistry. Condensation of 2-phenoxyaniline with 2,5-dimethoxybenzaldehyde in methanol at room temperature followed by reduction gave *N*-(2,5-dimethoxybenzyl)-2-phenoxyaniline (**7**) (Scheme 1). Treatment of **7** with bromoacetyl bromide in the presence of triethylamine gave the bromo precursor (**8**), required for the radiosynthesis of [^{18}F]**9**. Reference ligand **9** was prepared by treating **8** with dry potassium fluoride in di(ethylene glycol) at 150 °C. Similar bromoacetylation of 2-phenoxyaniline followed by fluorination gave the metabolite **11** (Scheme 2).

Scheme 2. Synthesis of **11** and [^{18}F]**11** [a]

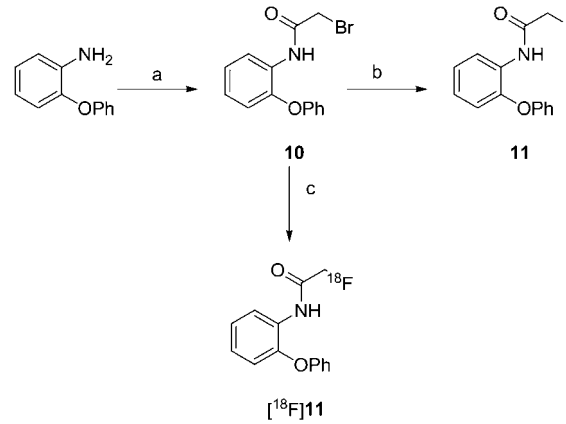

[a] Reaction conditions and yields: (a) bromoacetic anhydride, AcOH, Et_3N, rt, 2 h; 80%; (b) KF, ethylene glycol, 150 °C, 2 h; 65%; (c) [^{18}F]fluoride ion, MeCN, K 2.2.2, K_2CO_3; 160 °C, RCY 26−30%.

Table 1. Affinities (K_i values) of Ligands for PBR in Brain Homogenates from Rat, Monkey, and Human (Determined with [^{3}H]PK 11195 as Radioligand)

	PBR affinity (K_i, nM)[a]		
ligand	rat	monkey	human
1	0.0726 ± 0.0036	0.230 ± 0.011	0.242 ± 0.016
9	0.180 ± 0.007	0.318 ± 0.018	0.997 ± 0.070

[a] Values are mean ± SD (n = 6).

Binding Assays. The affinities of ligand **9** for PBR in rat, monkey, and human mitochondrial fractions were high and similar to those of **1** (Table 1). Ligands **1** and **9** showed a small interspecies variability in affinity for PBR, with that for human tissue being somewhat lower than for monkey or rat.

Experimental Radiosynthesis of [^{18}F]9 and [^{18}F]11. Experimentally, [^{18}F]**9** was obtained in almost quantitative (97%)

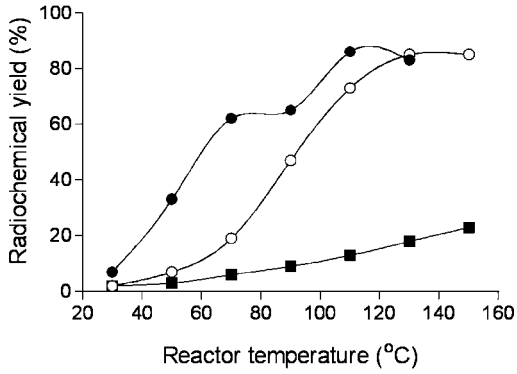

Figure 1. Temperature dependence of decay-corrected radiochemical yields of [^{18}F]**9** prepared in anhydrous MeCN (●) or MeCN containing 0.3% v/v H_2O (○), and of [^{18}F]**11** prepared in anhydrous MeCN within a microfluidic device using two 2 m-coiled microreactors (■).

decay-corrected radiochemical yield (RCY) from the reaction of cyclotron-produced [^{18}F]fluoride ion with **8** in pyrex glass vials.

In the microfluidic apparatus, [^{18}F]**9** was produced in higher RCY in anhydrous acetonitrile than in slightly wet acetonitrile at temperatures below 90 °C (Figure 1). However, this difference disappeared when the temperature of the reactor was raised above 110 °C. RCY reached 85% at 110 °C; further temperature increase gave no improvement. At a set temperature, excess **8** (i.e., [^{18}F]F^- to **8** solution volume ratio = 1:2) gave much higher radiochemical yield than excess [^{18}F]F^-−K^+−K 2.2.2 (i.e., [^{18}F]F^- to **8** solution volume ratio = 2:1). For example, at 90 °C in anhydrous acetonitrile, RCYs were 77 versus 44%, while in acetonitrile containing trace water (0.3% v/v), they were 79 versus 29%.

The RCY of [^{18}F]**11** in the microfluidic apparatus was substantially lower than for [^{18}F]**9** over the temperature range 30−150 °C under comparable conditions (Figure 1).

Microfluidic Production of [^{18}F]9 for Intravenous Injection into Rat. RCYs of radiochemically pure [^{18}F]**9** ranged from 69 to 76% for reactions conducted at 110 °C.

Microfluidic Production of [^{18}F]11 for Intravenous Injection into Rat. RCYs of radiochemically pure [^{18}F]**11** ranged from 26 to 30% for reactions conducted at 160 °C.

Automated Production of [^{18}F]9 for Intravenous Injection into Monkey. [^{18}F]**9** was produced automatically within a lead-shielded hot-cell from high levels of cyclotron-produced [^{18}F]fluoride ion (∼300 mCi) in either a commercial apparatus (TRACERlab FX_{F-N}) or a Synthia device[41] equipped with a microwave heater.[42] Purification of [^{18}F]**9** was achieved by single-pass HPLC. From the Synthia apparatus, [^{18}F]**9** was obtained in high radiochemical purity (100%) and chemical purity. Specific radioactivity ranged from 3.4 to 9.0 Ci/μmol at the end of synthesis at about 180 min from the end of radionuclide production. The average isolated RCY of [^{18}F]**9** was 12.2% (n = 6).

Measurement of LogD and Computation of cLogD and cLogP. The measured LogD value and computed cLogP and cLogD values of **9** were 4.05 ± 0.02 (n = 6), 4.37 and 4.38, respectively.

Stability of [^{18}F]9 in Monkey Whole Blood and Plasma, and in Buffer. After incubation with monkey whole blood and plasma for at least 45 min at room temperature, [^{18}F]**9** was 95.5 ± 3.2% (n = 5) and 97.2 ± 1.0% (n = 6) unchanged, respectively. [^{18}F]**9** was stable in sodium phosphate buffer (0.15 M, pH 7.4) for longer than 2 h at room temperature.

Distribution of [^{18}F]9 in Monkey Blood and Plasma Free Fraction. In monkey blood, [^{18}F]**9** distributed 93.4 ± 0.3% to cells and 6.6 ± 0.4% to plasma (n = 4). The plasma free fraction (f_P) of [^{18}F]**9** in two monkeys was 3.5 ± 0.2% (n = 9) and 1.34 ± 0.1% (n = 3) and in human pooled plasma was 0.70 ± 0.03% (n = 3).

PET Imaging of [^{18}F]9 in Monkeys. After injection of NCA (no-carrier-added) [^{18}F]**9** into monkeys, radioactivity entered the brain well with peak uptake occurring in all PBR-containing regions between 27 and 72 min after injection (Figure 2A). Maximal uptake occurred in choroid plexus of fourth ventricle (350 ± 116% SUV; n = 3). Subsequent washout of radioactivity from all PBR-containing regions was quite slow. In a repeat experiment in one monkey, in which PBR receptors were preblocked by administration of **1**, the kinetics of brain radioactivity was strikingly different. Radioactivity was rapidly taken into all examined brain regions, but to a much higher level than in the baseline experiment, and then washed out rapidly to a low common level (Figure 2B). In a displacement experiment in another monkey, administration of **1** at 60 min after radioligand caused a rapid decline in radioactivity in all PBR-containing regions to a low common level (Figure 2C).

Average PET images of monkey brain acquired over a late period (60−120 min) after injection of [^{18}F]**9** (Figure 3, upper row) were coregistered with MR images (Figure 3, lower row) and displayed a high level of radioactivity, especially in the choroid plexus of fourth ventricle, cerebellum and striatum, and intermediate levels in frontal, parietal, temporal, and occipital cortex. Corresponding scans from the preblock experiment showed a low uniform distribution of radioactivity (Figure 3). No radioactivity accumulated in bone (skull).

Emergence of Radiometabolites of [^{18}F]9 in Monkey Plasma In Vivo. After administration of [^{18}F]**9** into monkey, radioactivity (and hence radioligand) cleared rapidly from plasma (Figure 4). HPLC analyses of plasma from four monkeys revealed [^{18}F]**9** eluting at 6.64 ± 0.25 min, a major radiometabolite at 2.47 ± 0.18 min, and a minor radiometabolite at 4.38 ± 0.90 min (n = 64). The latter was never higher than 4% of the total plasma radioactivity except in one monkey, where it reached 8% in one plasma sample at 60 min after injection. The 64 observations were obtained from three monkeys on which four studies were performed. Recoveries of radioactivity from plasma into supernatant acetonitrile for HPLC analysis averaged 93.4 ± 2.3% (n = 64). Monkey plasma became composed equally of radiometabolite and [^{18}F]**9** at 31.1 ± 14.7 min (n = 3) after radioligand injection in baseline experiments and at the much shorter time of 4.0 min in the preblock experiment (Figure 5). The concentration of unchanged [^{18}F]**9** in plasma (%SUV) was vastly higher in the preblock than in the baseline experiment, especially over the initial 10 min; in fact, peak values were nearly 18-fold higher in the preblock experiment (Figure 6).

Stability of [^{18}F]9 to Rat Brain In Vitro. [^{18}F]**9** was found to be >99.2% unchanged when incubated with brain homogenate at 37 °C for up to 60 min. Recoveries of radioactivity from homogenates for analyses were >82%.

Emergence of Radiometabolites of [^{18}F]9 in Rat Plasma, Brain, and Urine In Vivo. At 30 min after administration of NCA [^{18}F]**9** (1.36 Ci/μmol) to rat (mass dose of **9**, 0.85 μg/kg), the recoveries of radioactivity from plasma and brain homogenate samples into acetonitrile for analyses with HPLC were very high, namely 92.7% (n = 2) and 85.1% (n = 4), respectively. [^{18}F]**9** (t_R = 5.3 min in plasma analyses, 6.5 ± 1.2 min in brain analyses) represented 12.5 (n = 2) and 90.4 ± 0.2% (n = 4) of plasma and brain radioactivity, respectively.

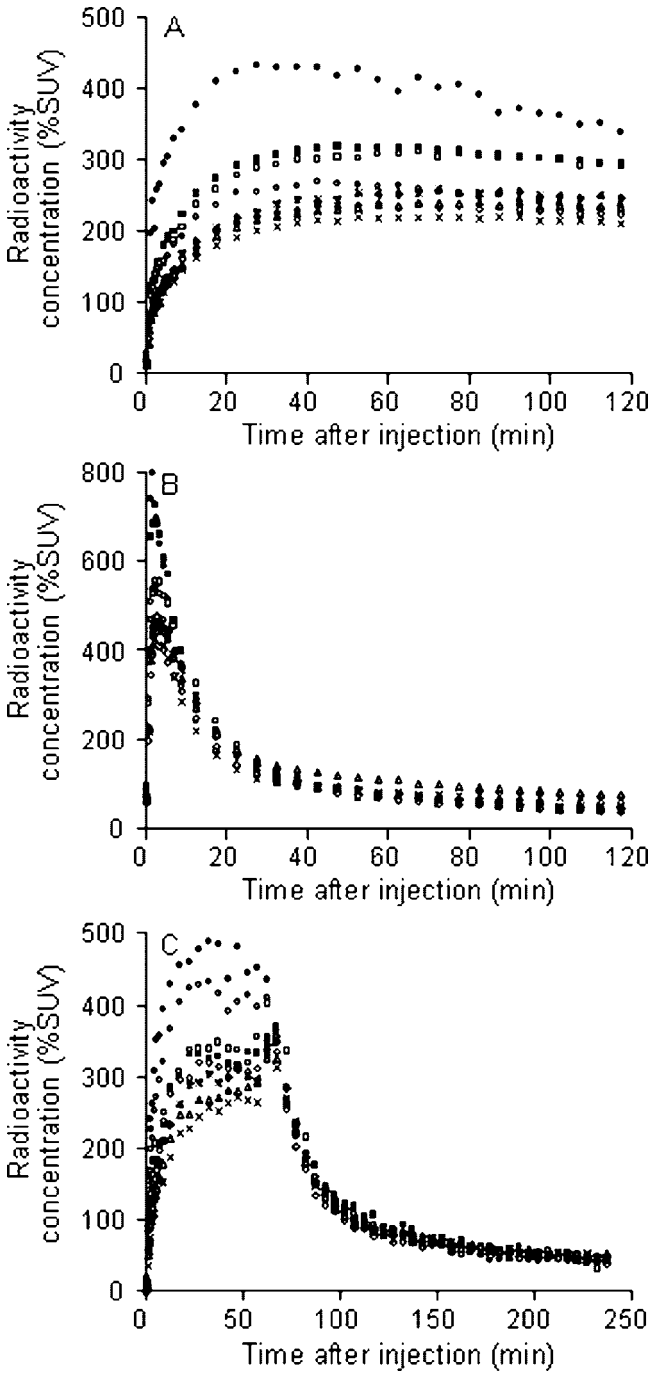

Figure 2. Rhesus monkey brain time-activity curves after intravenous injection of [^{18}F]**9** (5.80 mCi with 3.91 μg of **9**) alone (A), intravenous injection of **1** (3 mg/kg) in the same monkey at 24 min before [^{18}F]**9** (5.09 mCi, with 4.58 μg of **9**) (B), and intravenous injection in a different monkey of [^{18}F]**9** (1.28 mCi, with 1.75 μg of **9**) followed at 60 min later with **1** (3 mg/kg) (C). Key: fourth ventricle of choroid plexus (●), striatum (■), thalamus (□), cerebellum (○), frontal cortex (×), temporal cortex (△), parietal cortex (*), and occipital cortex (◇).

The remainder of radioactivity was predominantly polar radiometabolite(s), eluting at the void volume (t_R = 2.0 min). In a second rat, administered with NCA [^{18}F]**9** at a somewhat lower specific radioactivity (mass dose of **9**, 3.78 μg/kg), [^{18}F]**9** represented 44.6, 37.6, and 5.7% of radioactivity in plasma at 7.3, 10.9, and 94.3 min, respectively and 39.2% of radioactivity in brain at time of sacrifice (95 min) (n = 2 for all measures). The remainder of radioactivity in plasma and brain was mainly polar radiometabolite(s) (t_R = 2.0 min). A minor radiometabolite (<5% of total radioactivity) eluted ahead of [^{18}F]**9** at t_R = 3.5 min. In this experiment, recoveries of radioactivity into acetonitrile analytes were 93.0 ± 0.8% for plasma and 81.8% for brain.

In the two rats administered with carrier-added (CA) [^{18}F]**9**, unchanged [^{18}F]**9** represented 32.6 ± 2.5% of brain radioactivity and 14.2 ± 1.9% of plasma at time of sacrifice (60 min). Unchanged [^{18}F]**9** represented only 0.2 ± 0.1% of radioactivity in urine. The remainder of radioactivity in brain, plasma, and urine was dominated by polar radiometabolite(s). The minor radiometabolite represented <5, <3, and 9.9 ± 2.2% of radioactivity in brain, plasma, and urine, respectively. In this experiment, recoveries of radioactivity into acetonitrile analytes were 93.2 ± 1.0%, 91 ± 0.7%, and 80.3 ± 3.5% for plasma, brain, and urine, respectively.

LC-MS-MS Search for Metabolites of 9 Emerging in Rat Brain, Urine and Plasma in Vivo. Reference ligand **9** eluted with t_R = 12.9 min in LC-MS and showed an $[M + 1]^+$ ion at m/z = 396 and an adduct at m/z = 441. MS-MS analysis of this ion gave product ions m/z 258 and 151.

LC-MS-MS analyses of brain and plasma, sampled at 115 min after administration of **3** to rat, detected unchanged **9**. Unchanged **9** was not detected in urine. A knowledge-based metabolite search of the total ion chromatograms for brain, plasma, and urine detected an intense peak at 11.3 min for m/z 186 ion, consistent with $[M + H]^+$ for 2-phenoxyaniline, a possible metabolite of **9**. The MS−MS of this ion gave a product ion spectrum consisting of m/z 169, 168, 158, 108, and 93, which exactly matched that of reference 2-phenoxyaniline. This metabolite was also similarly detected and identified in plasma. The metabolite that would have been generated solely by *N*-deacetylation of **9**, namely **7**, was not detected in brain, urine or plasma. No metabolites from possible *O*-demethylation were detected.

Emergence of Radiometabolites of [^{18}F]11 in Rat Brain and Plasma In Vitro. Incubation of the synthesized radiometabolite, [^{18}F]**11,** with rat brain homogenate or rat whole blood for 30 min resulted in virtually complete conversion (>99.9%) into polar radiometabolite(s) that eluted at the solvent front on reverse phase HPLC.

Emergence of Radiometabolites of [^{18}F]11 in Rat Brain and Plasma Ex Vivo. At 30 min after administration of [^{18}F]**11** to rat, ex vivo analysis showed that radioactivity in brain and plasma was almost entirely (>99%) the polar radiometabolite(s) that eluted at the solvent front on reverse phase HPLC.

Evaluation of the Rat Brain Penetration of the Radiometabolite(s) of [^{18}F]11. The radiometabolite(s) of [^{18}F]**11** generated in rat blood in vivo were found to have a moderate presence in brain at 30 min (130% SUV uncorrected, 120% corrected for blood) after intravenous injection relative to their concentrations in blood (196% SUV) or plasma (226% SUV) at the same time.

Discussion

Our aim was to develop a sensitive and easily prepared ^{18}F-labeled ligand for PET imaging of brain PBR. High affinity is a primary requirement for a PET radioligand to exhibit high sensitivity.[43,44] Many high affinity *N*-acyl aryloxyanilide ligands, related to **1**, are known for PBR.[45−47] The reported structure-affinity data have indicated that the *N*-acyl function may be varied slightly without excessive detriment to binding affinity. We considered that the *N*-acyl function might be a favorable site for single-step introduction of fluorine-18 in our development of an ^{18}F-labeled PET ligand. For example, we had recently

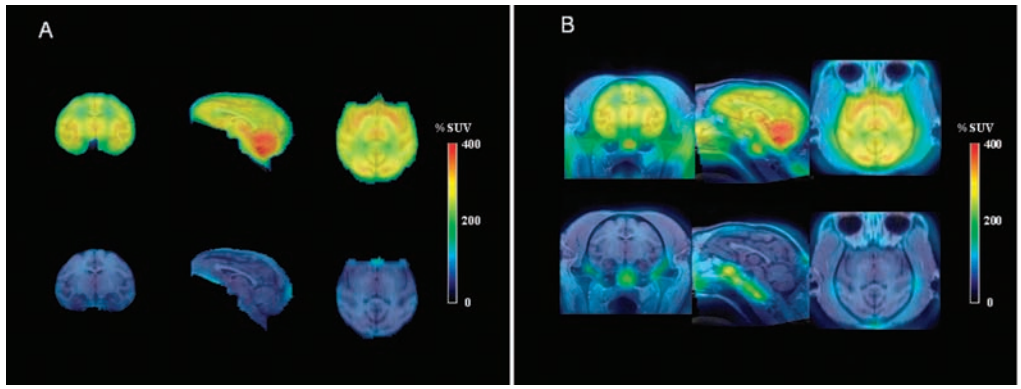

Figure 3. (A) In left to right order, average coronal, sagittal, and horizontal PET images of monkey brain, acquired between 60 and 120 min after intravenous injection of NCA [^{18}F]**9** (5.8 mCi) alone (upper row) and in the same monkey after preblock of PBR with **1** (3 mg/kg, iv) given 24 min before NCA [^{18}F]**9** (5.09 mCi) (lower row). (B) The same PET data have been superimposed on the corresponding MR images.

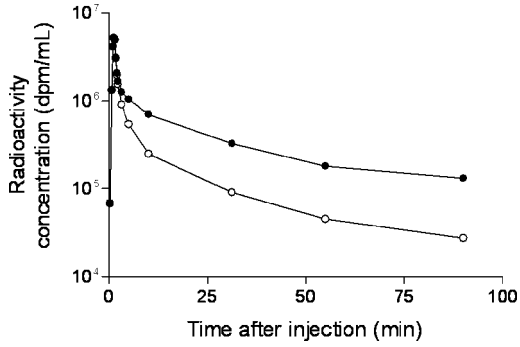

Figure 4. Time course of plasma concentration of total radioactivity (%SUV) (●) and unchanged [^{18}F]**9** (○) after intravenous injection of NCA [^{18}F]**9** into rhesus monkey.

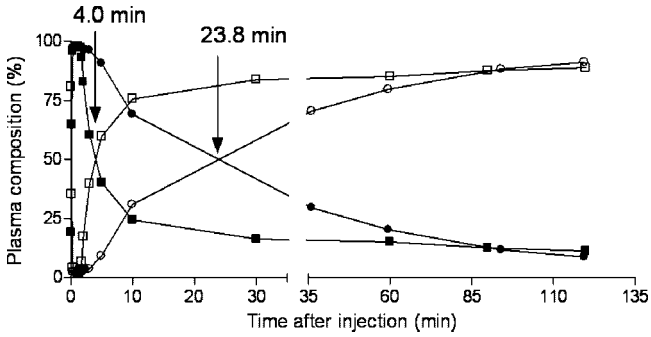

Figure 5. Time course of compositions of plasma radioactivity after injection of [^{18}F]**9** into the same rhesus monkey under baseline and PBR preblock conditions. (●) unchanged [^{18}F]**9** in baseline experiment; (○) radiometabolites in baseline experiment; (■) unchanged [^{18}F]**9** in preblock experiment; (□) radiometabolites in preblock experiment. Arrows indicate the times at which [^{18}F]**9** and its radiometabolite were equally present in these experiments.

shown that an *N*-fluoroacetyl group can be labeled efficiently with fluorine-18 by nucleophilic substitution in the corresponding *N*-bromoacetyl compound with NCA [^{18}F]fluoride ion.[48] We considered that simply switching the position of the fluorine atom in **1** (Chart 1) from the aryl ring to the *N*-acetyl group might provide a high affinity ligand for PBR. Furthermore, this switch was expected and then computed to have minimal effect on ligand lipophilicity, which is a key property influencing blood-brain barrier penetration, level of nonspecific binding, blood-protein binding, and metabolism.[43,44,49] Thus, cLogP and cLogD values for *N*-fluoroacetyl-*N*-(2,5-dimethoxybenzyl)-2-phenoxyaniline (**9**) were computed to be 4.37 and 4.38 and almost identical to those of **1** (each 4.27). These values are high

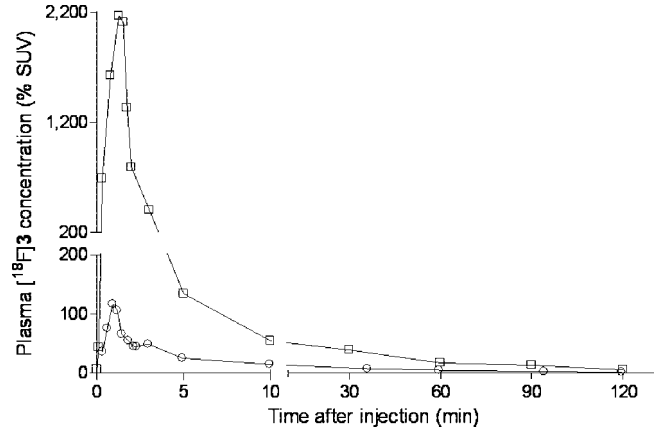

Figure 6. Time course of plasma concentration of [^{18}F]**9** (%SUV) after intravenous injection of [^{18}F]**9** in the baseline (○) and preblock experiment in the same monkey (□).

and above those normally considered ideal for achieving good brain penetration in PET radioligands without excessive nonspecific binding. Nevertheless, these values were not seen as problematic for the development of a PET radioligand because [^{11}C]**1** was already known to penetrate brain readily, as were [^{11}C]**2** ([^{11}C]PBR01) and [^{11}C]**3**,[26] which are also effective PBR radioligands based on a core aryloxyanilide structure (Chart 1). Therefore, we set out to prepare and test **9** as a potential ligand for PBR.

The synthesis of **9** was simply accomplished in high yield in three steps from commercially available materials and proceeded via the corresponding bromo compound (**8**) required for radiolabeling (Scheme 1). Ligand **9** was found to be selective for PBR[50] and to have high affinity for PBR across three species, namely rat, monkey, and human, with values comparable to those of the prototypical PBR ligand, **1** (Table 1). Only a small species variation in affinity was observed.

Experimentally, radioligand [^{18}F]**9** was easily prepared in a single step from the bromo precursor **8** and cyclotron-produced NCA [^{18}F]fluoride ion under conditions (MeCN, $KHCO_3$, 18-crown-6, trace water, 110 °C, 10 min) previously established for this type of radiosynthesis[48] (Scheme 1). Almost quantitative incorporation of [^{18}F]fluoride ion was achieved experimentally.

The labeling reaction was investigated further in a commercial microfluidic device, which provided for well-controlled conditions (reaction stoichiometry, temperature, and transit time) and multiple reactions over a short time-span. In this apparatus, radiochemical yields of [^{18}F]**9** reached 85% at 110 °C, whether

reactions were performed in dry or slightly wet acetonitrile (Figure 1). The tolerance of a low level of water in this reaction suggests the precursor is highly reactive toward hydrated [^{18}F]fluoride ion.[51]

An attractive feature of the radiosynthesis of [^{18}F]**9** in the microfluidic device is the very low amount of precursor (40 μg each run) that was required in the reaction, which in turn diminished the amount of nonradioactive impurities that were produced. Reverse phase HPLC analysis of [^{18}F]**9** product with eluate monitored for absorbance at 230 nm revealed very few nonradioactive impurities, which were all at very low level. Hence, the microfluidic device was readily applied to producing low activities of radiochemically pure [^{18}F]**9** for intravenous injection into rats. Similarly, useful activities of the later-discovered metabolite, [^{18}F]**11**, were produced in the microfluidic apparatus for injection into rats. However, radiochemical yields of [^{18}F]**11** were lower than for [^{18}F]**9** under comparable reaction conditions (Figure 1).

Radiochemistry was also readily adapted for the automated production of [^{18}F]**9** from high activities of [^{18}F]fluoride ion, first in a commercially available apparatus (TRACERlab FX_{F-N}; GE Medical Systems) under thermal labeling conditions and second within a Synthia device[41] equipped with a microwave-heated reactor.[42] Compound **8** was required to be of high purity and dryness for production of [^{18}F]**9**; we found **8** could be kept in this condition for several months by storage in a desiccator at room temperature. Single pass reverse phase HPLC was used to separate [^{18}F]**9**. Formulated [^{18}F]**9** was found to be radiochemically stable for at least 4 h. Stringent demands for radiochemical purity, chemical purity and specific radioactivity in [^{18}F]**9** were met with the Synthia process, which is now being used to produce [^{18}F]**9** for human use under an exploratory Investigational New Drug application from the U.S. Food and Drug Administration.

The single-step high-yield radiosynthesis of [^{18}F]**9** is a significant advantage over the radiosyntheses of the other two evaluated ^{18}F-labeled PBR radioligands known from the aryloxyanilide class, [^{18}F]**4** and [^{18}F]**5**, which preferably require two radiochemistry steps.[31] The alternative single-step radiosyntheses of these two radioligands gave erratic yields. The nonisolated radiochemical yield of [^{18}F]**9** also exceeds that of [^{18}F]**1** (46%).[34]

The lipophilicity ($LogD_{7.4}$) of **9** was measured with [^{18}F]**9** and found to be very close to the computed value (4.05 vs. 4.37). [^{18}F]**9** was found to be stable in whole monkey blood and plasma in vitro, in rat brain homogenate, and also in buffer. The distribution of [^{18}F]**9** in blood strongly favored uptake into cells. Much of this uptake is likely to be specific binding to PBR present in many blood cells,[52] including monocytes, lymphocytes, platelets, and erythrocytes.[53] The plasma free fraction (f_P) in monkey and human was low but still measurable with accuracy, as would be required for successful biomathematical modeling of acquired PET data.[44]

We assessed the radioligand behavior of [^{18}F]**9** in rhesus monkeys with PET. In three baseline experiments in which NCA [^{18}F]**9** was given alone, radioactivity was avidly taken into brain (Figure 2A). Maximal uptake occurred in choroid plexus of fourth ventricle, a region known to have high PBR density relative to other brain regions from in vitro autoradiography.[54] Progressively lower uptakes were seen in putamen, thalamus, cerebellum, and cortical regions. This distribution was similar to those seen in rhesus monkey for the PBR radioligands, [^{11}C]**2** and [^{11}C]**3**.[26] Radioactivity in all regions was well-retained throughout the experiments.

In a second PET experiment in one monkey, a high dose of **1** was given before administration of [^{18}F]**9** to presaturate[26] brain PBR. In this experiment, early maximal uptake of radioactivity across all inspected brain regions was substantially higher (Figure 2B) than that seen in the baseline experiment in the same monkey (Figure 2A). Uptake in all regions was followed by rapid continuous decline of radioactivity to a very low level (Figure 2B), indicating low and rapidly reducing nonspecific binding of radioactive species in brain.

Average PET images obtained under baseline conditions and coregistered with MR images detail the distribution of radioligand throughout monkey brain and feature especially high uptake in choroid plexus (Figure 3, upper row). Corresponding scans from the preblock experiment showed a low uniform distribution of radioactivity (Figure 3, lower row). Neither set of images showed a substantial uptake of radioactivity into skull (bone). Hence, [^{18}F]**9** does not defluorinate significantly in monkey. This may be a considerable advantage of [^{18}F]**9** over the previously reported radioligand, [^{18}F]**4** (Chart 1), which is rapidly defluorinated in mouse.[32]

Administration of the PBR-selective ligand **1** to a monkey at 60 min after [^{18}F]**9** caused an almost immediate and rapid decrease in radioactivity to a low common level in all inspected brain regions (Figure 2C). This confirmed the high selectivity of [^{18}F]**9** for binding to PBR in brain and the rapid washout of nonspecific binding. Because administration of **1** displaced a high proportion of radioactivity (e.g., up to 90% in choroid plexus, Figure 2C), it appears that nonpharmacologically active radiometabolite(s) could account for only a small proportion of radioactivity in monkey brain at 60 min. This observation is consistent with our ability to quantify the binding of [^{18}F]**9** to monkey brain PBR.[50]

The combined PET data imply a very high ratio of PBR-specific to nonspecific binding for [^{18}F]**9** in monkey baseline experiments, and point to the high sensitivity of this radioligand. Accurate quantification of the specific binding of [^{18}F]**9** requires sophisticated biomathematical modeling of the acquired PET data plus an accompanying measured arterial input function.[50] It should be noted that our previous PET studies with [^{11}C]**3** have revealed that even the low density of PBR in normal rhesus monkey brain[54] is about 20-fold higher than in normal human brain.[28,29] Our recent quantitative PET studies in normal monkey[50] and human (Fujimura et al., submitted) with [^{18}F]**9** also show this species difference. Hence, in human subjects, even small increases in [^{18}F]**9** binding to PBR, as may be expected at inflammatory lesions, should be easily detectable and quantifiable against a low background.

An understanding of the metabolism of a candidate PET radioligand can be important in establishing its worth for quantitative imaging. Ideally, the candidate radioligand should not give rise to radiometabolites that can enter brain significantly to sully the identity of the acquired PET signal. After administration of [^{18}F]**9** alone to monkey, radioactivity in plasma reduced quite slowly, while a decreasing proportion of this radioactivity was unchanged radioligand (Figure 4). The remainder of the radioactivity was composed mainly of a polar radiometabolite, as evidenced by its elution at the solvent front on reverse phase HPLC, plus a minor radiometabolite of intermediate retention time and lipophilicity. Half of the radioactivity in plasma became radiometabolite at, on average, 31 min after radioligand injection (Figure 5).

Measurements of unchanged [^{18}F]**9** in plasma revealed the vastly increased availability of unchanged [^{18}F]**9** in blood under the preblock condition compared to that under the baseline

Scheme 3. Summary of Metabolism of [^{18}F]**9** in rat in vivo

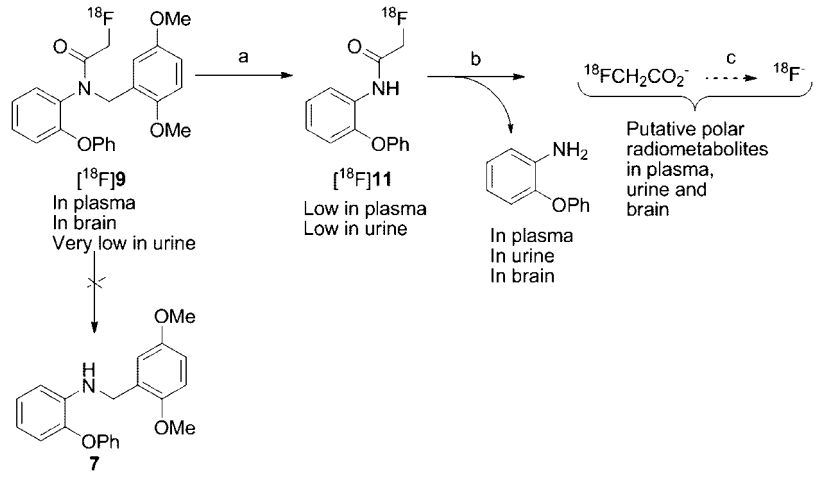

condition, especially during the early phase after radioligand injection (Figure 6). This increase is concluded to be due to the blockade of radioligand binding to abundant peripheral PBR receptors. A similar large increase in plasma radioligand concentration under PBR preblock conditions has been observed[26] for the related ^{11}C-labeled radioligand, [^{11}C]**3**. The preblock conditions, used in that study and here, have been shown with PET to block PBR receptors in the periphery (e.g., in kidney and lung).[27] Hence, the early higher brain uptakes of radioactivity in the preblock experiment (Figure 2B) than in the baseline experiment (Figure 2A) are explained by a much higher input of radioactivity into brain.

The preblock of all PBR receptors also influenced the emergence of radiometabolite in monkey plasma in that the time taken for radiometabolite to reach half of the radioactivity content was greatly reduced, for example, in one of the studied monkeys from 24 to 4 min (Figure 5). Similar effects of PBR blockade have been observed for [^{11}C]**2** and [^{11}C]**3**.[26] This effect may be due to early greater availability of parent radioligand to metabolizing enzyme(s) under the PBR preblock condition, i.e., under the preblock condition, the [^{18}F]**9** is not protected from metabolism by its specific binding to PBR receptors in brain and periphery.

Experiments were performed in rats to gain greater insight into the metabolism of [^{18}F]**9**. Radiometabolites appeared quite rapidly in rat plasma after the intravenous administration of [^{18}F]**9**. As in monkey, these radiometabolites consisted mainly of polar radiometabolite eluting at the solvent front on reverse phase HPLC and a minor radiometabolite eluting ahead of the unchanged [^{18}F]**9**. In urine, these radiometabolites were abundant, whereas parent radioligand was relatively very low. [^{18}F]**9** and its radiometabolites were found in brain, with their relative proportions dependent on time from injection and the specific radioactivity of the administered radioligand. For the administration of high specific radioactivity radioligand with brain measured at 30 min, the proportion of radioactivity in brain represented by unchanged [^{18}F]**9** was high (>90%). This is an encouraging finding for imaging in higher species and human subjects, which are generally considered to be less rapidly metabolizing. In more detailed studies, we have found that the uptake of [^{18}F]**9** in monkey[50] and human brain (Fujmura Y. et al., submitted) may indeed be quantified satisfactorily with compartmental modeling and that the ingress of radiometabolites into brain is not greatly problematic for such quantitation. At later times, radiometabolites represented an increasing percentage of radioactivity in brain. This was also the case for [^{18}F]**9** administered at lower specific radioactivity. An interpretation of this finding is that brain PBR are less available for binding unchanged [^{18}F]**9** when at low specific radioactivity, while the nonspecific binding of unchanged [^{18}F]**9** remains low. Also, as previously mentioned, [^{18}F]**9** appears to be less protected from peripheral metabolism at lower specific radioactivity; this results in greater early input of radiometabolites into brain.

Our ex vivo search for the metabolites of **9** in rat with LC-MS-MS detected unchanged **9** in plasma and brain but not urine, and also 2-phenoxyaniline in plasma, brain, and urine. No other possible metabolites were detectable, including **7**, which would need to arise by a single step of deacylation. Therefore, we hypothesized that 2-phenoxyaniline was generated by debenzylation of **9** to compound **11** followed by deacylation (Scheme 3). In accord with this hypothesis, [^{18}F]**9** would give [^{18}F]**11** as a radiometabolite (Scheme 3). This hypothesis was strongly supported when synthesized **11** and [^{18}F]**11** were found to coelute with the low level intermediate radiometabolite of [^{18}F]**9** on reverse phase HPLC. We therefore further investigated the behavior of [^{18}F]**11** in rat blood and brain homogenate in vitro and in rat in vivo. [^{18}F]**11** was found to be almost completely metabolized to polar radiometabolite(s) when incubated for 30 min with rat whole blood or rat brain homogenate. At 30 min after administration of [^{18}F]**11** to rat in vivo, polar radiometabolite(s) also emerged rapidly in plasma, brain, and urine. We postulate that the polar radiometabolite(s) arise first through deacylation of [^{18}F]**11** to polar [^{18}F]fluoroacetate. [^{18}F]Fluoroacetate has been proposed as a radiotracer for prostate tumors[55] and is known to be further metabolized to [^{18}F]fluoride ion in mouse and rat but not baboon.[56] The polar radiometabolites of [^{18}F]**9** seen in monkey and in rat are therefore likely to be [^{18}F]fluoroacetate and/or its radiometabolites. We found a low level of radioactivity in rat brain (120% SUV) at 30 min after the isolated polar radiometabolite(s) of [^{18}F]**11** from rat were injected into another rat.

Conclusions

Compound **9** is a selective ligand for PBR with high affinity across three species, rat, monkey, and human. Radioligand [^{18}F]**9** is easily prepared in high radiochemical yield and specific radioactivity from the easily obtained bromo precursor, **8**. [^{18}F]**9** is avidly taken up by monkey brain and provides a high ratio of PBR-specific to nonspecific binding. In monkey and in rat, [^{18}F]**9** shows no evidence of significant defluorination and gives mainly polar radiometabolite. [^{18}F]**9** is therefore a promising

radioligand for the future study of PBR in human subjects. Preliminary evaluation of this radiotracer in human subject has been performed under an exploratory-IND from the FDA (Fujimura et al. submitted).

Experimental Section

Materials. Poly(ethyleneimine) and PK 11195 were purchased from Sigma (St. Louis, MO). **1** was synthesized from commercially available 2,5-difluoronitrobenzene, as described previously.[45] An ethanolic solution of [*N-methyl*-^{3}H]PK 11195 (>97% radiochemical purity; 83.5 Ci/mmol) was purchased from Perkin-Elmer (Wellesley, MA, USA). Other chemicals were purchased from Aldrich Chemical Co. (Milwaukee, WI) and used as received. All animals used in this study were handled in accordance with the *Guide for the Care and Use of Laboratory Animals*[57] and the National Institute of Mental Health Animal Care and Use Committee. Human brain tissue was obtained from the Clinical Brain Disorders Branch, National Institute of Mental Health, and experiments with this material were performed under the regulations of the Ethics Committee of the National Institutes of Health.

General Methods. γ-Radioactivity from ^{18}F was measured with a calibrated dose calibrator (Atomlab 300; Biodex Medical Systems, USA) or for low levels (<1 μCi) with a well-type γ-counter (model 1080 Wizard; Perkin-Elmer; Boston, MA) having an electronic window set between 360 and 1800 keV. ^{18}F radioactivity measurements were corrected for background and physical decay. All radiochemistry with fluorine-18 was performed in lead-shielded hot-cells. ^{3}H was measured with a liquid scintillation counter (Tri-Carb; Perkin-Elmer). ^{1}H- (400 MHz), ^{13}C- (100 MHz), and ^{19}F-NMR (376.49 MHz) spectra were recorded at room temperature on an Avance-400 spectrometer (Bruker; Billerica, MA). ^{1}H and ^{13}C chemical shifts are reported in δ units (ppm) downfield relative to the chemical shift for tetramethylsilane and ^{19}F chemical shifts relative to $CFCl_3$. Abbreviations br, s, d, t, and m denote broad, singlet, doublet, triplet, and multiplet, respectively.

High resolution mass spectra (HRMS) were acquired from the Mass Spectrometry Laboratory, University of Illinois at Urbana−Champaign (Urbana, IL) under electron ionization conditions using a double-focusing high-resolution mass spectrometer (Autospec; Micromass Inc., USA).

LC-MS and LC-MS-MS for compound characterization and for the analyses of biological samples were performed on a LCQ Deca instrument (Thermo Fisher Scientific Corp., Waltham, MA) equipped with a Synergi Fusion-RP column (4 μm, 150 mm × 2 mm; Phenomenex, Torrance, CA), as described previously.[26] For metabolite identification, the chromatogram was searched for all ions in the *m*/*z* range 150−750, to cover all ions from possible metabolites.

[^{18}F]**9** and its radiometabolites from samples of biological material were analyzed with HPLC on a Nova-Pak C18 column (4 μm, 100 mm × 8 mm; Waters Corp., USA) housed in a radial compression module (RCM 100) and eluted with MeOH:H_2O:Et_3N (75:25:0.1 by vol.) at 1.5 mL/min. Elution of all radioactivity from the column during each analysis was confirmed by subsequent injection of methanol (2 mL) and observation of no more radioactivity elution. The same HPLC method was applied to determine the radiochemical purities of [^{18}F]**9** preceding lipophilicity determinations and for the determination of radiochemical stability in various media (see below).

Melting points were measured with a Mel-Temp manual melting point apparatus (Electrothermal; Fisher Scientific), and were uncorrected.

***N*-(2,5-Dimethoxybenzyl)-2-phenoxyaniline (7).**[47] A solution of 2,5-dimethoxy-benzaldehyde (0.9 g; 5.4 mmol) and 2-phenoxyaniline (1.0 g; 5.4 mmol) in methanol (6 mL) was stirred for 24 h at room temperature. Then sodium borohydride (0.75 g; 20 mmol) was added slowly and the mixture stirred for 1 h. Aqueous acetic acid (16 mL; 5% v/v) was added dropwise. The mixture was stirred at room temperature for 30 min and then extracted thrice with EtOAc. The combined organic layers were washed with saturated aqueous $NaHCO_3$ and then brine, dried over $MgSO_4$, filtered, and concentrated in vacuo. The residue was purified on silica gel (hexane, EtOAc, 98:2 v/v) to give **7** (1.35 g, 75%). ^{1}H NMR ($CDCl_3$) δ 3.69 (3H, s), 3.70 (3H, s), 4.34 (2H, s), 4.70 (1H, s), 6.25−7.05 (10H, m), 7.25−7.32 (3H, m). ^{13}C NMR ($CDCl_3$) δ 43.08, 55.69, 111.07, 112.15, 112.18, 114.87, 116.88, 117.13, 119.64, 122.51, 125.09, 128.47, 129.66, 140.64, 142.95, 151.51, 153.56, 157.83. LC-MS, *m*/*z* = 336.0 [M + H]$^+$. HRMS, *m*/*z* = 336.1586 [M + H]$^+$, calcd for $C_{21}H_{22}NO_3$ [M$^+$ + H], 336.1600.

***N*-Bromoacetyl-*N*-(2,5-dimethoxybenzyl)-2-phenoxyaniline (8).** Bromoacetyl bromide (0.288 mL; 3.3 mmol) was slowly added to a solution of **7** (1.0 g; 3.0 mmol) and triethylamine (0.5 mL; 3.3 mmol) in dichloromethane (5 mL) at 0 °C. The mixture was stirred for 1 h at room temperature and then poured into water and extracted with dichloromethane. The combined organic layers were washed successively with hydrochloric acid (0.5 M), saturated $NaHCO_3$ solution, and saturated brine and then dried over $MgSO_4$ and concentrated to give **8** as a heavy oil (1.0 g, 73%); TLC (silica gel; hexane/EtOAc, 60:40 v/v, R_f = 0.38). Repeated recrystallization of the oil was from methanol−water (95/5 v/v) and finally absolute ethanol gave **8** as thin colorless needles; mp, 72 °C. ^{1}H NMR ($CDCl_3$) δ 3.53 (3H, s), 3.67 (3H, s), 3.79 (2H, d, *J* = 2.7 Hz), 4.69 (1H, d, *J* = 14.7 Hz), 5.19 (1H, d, *J* = 14.7 Hz), 6.65−6.75 (m, 2H), 6.83−7.02 (m, 4H), 7.11−7.27 (m, 2H), 7.30−7.38 (m, 2H). ^{13}C NMR ($CDCl_3$) δ 27.74, 46.89, 55.72, 55.81, 111.49, 113.88, 115.95, 118.16, 119.39, 123.14, 124.28, 125.78, 129.65, 129.94, 130.35, 131.51, 151.83, 153.53, 155.66, 166.91. LC-MS [M + H]$^+$, 456.08; HRMS, *m*/*z* = 456.0810 [M + H]$^+$, calcd for $C_{23}H_{23}BrNO_4$ [M + H]$^+$, 456.0810. Purity by LC: 100%.

***N*-Fluoroacetyl-*N*-(2,5-dimethoxybenzyl)-2-phenoxyaniline (9).** A mixture of **8** (0.80 g; 1.7 mmol), dry potassium fluoride (0.25 g; 4.3 mmol), and di(ethylene glycol) (5 mL) was stirred, heated rapidly to 150 °C, and kept at this temperature for 4 h. The reaction mixture was then cooled, diluted with water (10 mL), and extracted with ethyl acetate (3 × 10 mL). The combined organic layers were washed with sodium bicarbonate solution (5% w/v; 10 mL), dried over $MgSO_4$, filtered, concentrated, and purified on silica gel with hexane/ethyl acetate to give **9** as a viscous pink oil (0.6 g, 95%). TLC (silica gel, hexane-EtOAc, 60:40 v/v, R_f = 0.27). ^{1}H NMR ($CDCl_3$) δ 3.50 (3H, s), 3.67 (3H, s), 4.71 (2H, d, *J* = 47.2 Hz), 4.79 (1H, d, *J* = 14.2 Hz), 5.15 (1H, d, *J* = 14.2 Hz), 6.66−7.36 (12H, m). ^{13}C NMR ($CDCl_3$) δ 46.18, 55.67, 55.79, 77.99, 79.75, 111.50, 113.89, 116.61, 118.15, 119.38, 123.22, 124.33, 125.55, 129.46, 129.88, 129.95, 130.39, 151.99, 153.49, 153.79, 155.56, 166.99. ^{19}F NMR ($CFCl_3$) δ: − 227.10. LC-MS, *m*/*z* = 396.15 [M + H]$^+$. HRMS, *m*/*z* = 396.1616 [M + H]$^+$, calcd $C_{23}H_{23}FNO_4$ [M + H]$^+$, 396.1611. Purity by LC: 100%.

2-Bromo-*N*-(2-phenoxyphenyl)acetamide (10). Bromoacetic anhydride was added dropwise to a solution of 2-phenoxyaniline (1.0 g, 5.4 mmol) in glacial acetic acid (5 mL) and the reaction mixture stirred for 2 h at room temperature. Acetic acid was removed under reduced pressure. Aqueous NaOH (5 mL, 1 M) was added to the residue and the product was extracted with dichloromethane (3 × 10 mL). The organic layer was washed with water, dried over $MgSO_4$, filtered, and concentrated under vacuum. Flash chromatography on silica gel (hexane/ethyl acetate, 80:20 v/v) gave **10** (1.31 g; 80%) as a heavy colorless oil. ^{1}H NMR ($CDCl_3$) δ: 3.98 (s, 2H), 6.89 (dd, 1H, J_1 = 8.12, J_2 = 1.44 Hz), 7.04 (m, 3H), 7.14 (m, 2H), 7.36 (dt, 2H, J_1 = 7.48 and J_2 = 1.08 Hz), 8.39 (dd, 1H, J_1 = 8.08 and J_2 = 1.56 Hz), 8.79 (s, 1H). ^{13}C NMR ($CDCl_3$) δ: 28.01, 116.47, 116.94, 119.08, 122.46, 122.53, 123.54, 127.45, 128.44, 1244.37, 154.72, 161.83. LC-MS, *m*/*z* = 306 [M + H]$^+$. HRMS (*m*/*z*, ESI); [M + H]$^+$ calcd for $C_{14}H_{13}NO_2Br$ 306.0130, found 306.0116.

2-Fluoro-*N*-(2-phenoxyphenyl)acetamide (11). A mixture of compound **10** (0.5 g, 1.63 mmol) and dry potassium fluoride (0.24 g, 4.1 mmol) was suspended in ethylene glycol (5 mL). The suspension was stirred and heated rapidly to 150 °C and kept at this temperature for 2 h. The reaction mixture was cooled, diluted with water (10 mL), and extracted with toluene (2 × 10 mL). The organic layer was washed with sodium bicarbonate solution (5%

w/v; 10 mL), dried over $MgSO_4$, filtered, and concentrated. Chromatography on silica gel (hexane/ethyl acetate, 90:10 to 80:20 v/v) gave **11** (260 mg, 65%) as a peach-colored powder; mp: 75−77 °C. ^{1}H NMR ($CDCl_3$) δ: 4.95 (d, 2H, J = 47.3 Hz), 6.88 (dd, 1H, J_1 = 8.08, J_2 = 1.48 Hz), 7.05 (m, 3H), 7.15 (m, 2H), 7.37 (dt, 2H, J_1 = 7.48 and J_2 = 2.45 Hz), 8.45 (dd, 1H, J_1 = 8.04 and J_2 = 1.64 Hz), 8.59 (s, 1H). ^{13}C NMR ($CDCl_3$) δ: 79.92 (d, J_{C-F} = 188.46 Hz), 117.48, 118.55, 120.75, 123.70, 123.87, 124.64, 128.07, 129.76, 145.84, 155.93, 165.29 (d, J_{CO-F} = 161.16 Hz). ^{19}F-NMR ($CFCl_3$) δ: −222.18. LC-MS, m/z = 246 $[M + H]^+$. HRMS (m/z, ESI); $[M + H]^+$ calcd for $C_{14}H_{13}NO_2F$ 246.0925, found 246.0930.

Binding Assays of 9. Crude mitochondrial fractions from rat whole brain were prepared as described previously.[58] Monkey mitochondrial fraction from frozen samples of the temporal and parietal lobes, and human mitochondrial fraction from frozen brain tissue samples were prepared in the same manner. Competitive binding assays were performed with [^{3}H]PK 11195 as reference radioligand as described previously.[26]

Production of [^{18}F]Fluoride Ion. NCA [^{18}F]fluoride ion was produced with the ^{18}O(p,n)^{18}F reaction by irradiation of [^{18}O]water (95 atom %; 1.8 mL) with protons (14.1 MeV, 20−25 μA) generated with a PETtrace cyclotron (GE, Milwaukee, WI). Generally, this method produced [^{18}F]fluoride ion with a specific radioactivity exceeding 10 Ci/μmol.

Experimental Radiosynthesis of [^{18}F]9 and [^{18}F]11. A glass reaction vial (5 mL; V-vial) was loaded with an aqueous solution (10 μL) of $KHCO_3$ (0.7 mg; 7 μmol) plus a solution of 18-crown-6 (1.7 mg; 6.4 μmol) in acetonitrile (0.15 mL). [^{18}F]Fluoride ion (<2 mCi) in [^{18}O]water (20 μL) was added and the solvent evaporated under reduced pressure (controlled with a bleed of nitrogen) while heating at 110 °C (oil bath). Water was removed during three cycles of addition-evaporation of acetonitrile (0.3 mL each cycle). A solution of water (1 μL; 56 μmol) in acetonitrile (0.5 mL) was added to the dry residue, followed by addition of **8** (3 mg; 6.6 μmol) in acetonitrile (0.15 mL). The reaction vial was sealed, heated at 110 °C for 10 min, and then cooled to room temperature before analysis by radio-HPLC.[48]

This labeling reaction was further investigated in a commercial microfluidic device (NanoTek; Advion, Louisville, TN), which provides for well-controlled stoichiometry between precursor **8** and [^{18}F]fluoride ion at set flow rates and temperatures. NCA [^{18}F]fluoride ion in [^{18}O]water was first adsorbed onto a small MP-1 cartridge (ORTG, TN), then released with a solution of K_2CO_3 (5.5 mg/mL) and K 2.2.2 (30 mg/mL) in MeCN-H_2O (9:1 v/v; 150 μL) into a 5-mL V-vial. The solution was dried by two cycles of azeotropic evaporation with acetonitrile at 100 °C. The dry [^{18}F]F^--K^+-2.2.2 solution and precursor **8** (1.0 mg), both in acetonitrile (255 μL), were loaded into separate storage loops of the microreactor apparatus. For reaction condition optimization, 10 μL of solution from each loop was infused into the coiled microreactor (length, 2 m × 2 m; i.d., 100 μm) at different flow rates and temperatures. The reactor was heated for at least 5 min before the reagents were dispensed so that the reaction temperature was as close as possible to the heater temperature. The reaction was quenched by diluting the reactor output with H_2O-MeCN mixture (1:1 v/v; 1 mL) at room temperature. A portion (50−70 μL) of the diluted solution was analyzed by radio-HPLC with a Luna hexyl-phenyl column (3 μm, 100 Å, 150 mm × 4.6 mm; Phenomenex) eluted with aqueous ammonium formate (10 mM, in H_2O-MeCN, 40: 60 v/v) at 1 mL/min. [^{18}F]**9** eluted at 7.2 min. RCYs were calculated from the radio-HPLC analyses and were validated by collecting and measuring the corresponding HPLC fraction in selected samples. The reaction of **10** with [^{18}F]fluoride ion to produce [^{18}F]**11** was investigated in the same manner.

Microfluidic Production of [^{18}F]9 for Intravenous Injection into Rats. In the Nanotek apparatus, an acetonitrile solution (20 μL) of [^{18}F]F^--K^+-2.2.2 (∼1.2 mCi/mL), prepared as described above, was dispensed from one reagent loop and an acetonitrile solution of precursor **8** (4.2 mg/mL; 20 μL) from the other, each at 10 μL/min, into the microreactor (length, 4 m) at 110 °C. The collected reaction mixture was purified by reverse phase HPLC (conditions identical to the analytical conditions described above) and the [^{18}F]**9** fraction (6−7.5 min) was collected (∼1.5 mCi). The process was repeated thrice, and the combined [^{18}F]**9** solution diluted with water (15 mL), passed into a reverse phase column (3-mL size, SPEC C18AR; Varian, USA), and washed with water (10 mL). [^{18}F]**9** was eluted from the C18AR column with ethanol (250 μL) and diluted with saline (1.8 mL) to give [^{18}F]**9** for injection in saline containing ethanol (10% v/v).

Microfluidic Production of [^{18}F]11 for Intravenous Injection into Rats. The procedure for the production of [^{18}F]**9** was modified to use **10** as precursor. [^{18}F]**11** was separated on a Luna C18 column (250 mm × 4.6 mm; Phenomenex) eluted with a gradient of 25 mM $HCOONH_4$-MeCN increasing from 50% MeCN to 60% over 15 min and then maintained at 60% for 4 min (t_Rs 12.0 and 15.2 min for [^{18}F]**11** and **10**, respectively).

Automated Production of [^{18}F]9 for Intravenous Injection into Monkey. Productions were performed automatically within a lead-shielded hot-cell.

A commercial automated apparatus, namely the TRACERlab FX_{F-N} (GE Medical Systems, USA), was used initially. This apparatus is designed for performance of single-step reactions with [^{18}F]fluoride ion and for purification and formulation of radioactive product. In this apparatus, aqueous [^{18}F]fluoride ion (∼300 mCi) was dried by cycles of addition and evaporation of acetonitrile and complexed with K^+-K^+-2.2.2. This complex was reacted with precursor **8** (0.8−1.2 mg) at 100 °C for 20 min. [^{18}F]**9** was purified by injection (5 mL sample loop) into a semipreparative Luna C18 column (10 μm, 10 mm × 250 mm; Phenomenex) eluted at 4.5 mL/min with a mixture of (A) 50 mM ammonium formate (pH 6) and (B) 50 mM ammonium formate in MeCN (25:75, v/v) according to the program 57% B for 2 min, increasing to 62% B over 8 min and slow increase to 67% B for 40 min. The fraction containing [^{18}F]**9** (t_R = 25 min) was collected in water (100 mL). This solution was passed through a C-18 Sep-Pak and the trapped [^{18}F]**9** eluted with ethanol (1 mL) into a sterile flask loaded with saline (9 mL).

The production of [^{18}F]**9** was later performed in a Synthia apparatus adapted to use microwave irradiation for the labeling reaction. A microwave reactor (model 521; Resonance Instruments Inc., Skokie, IL) was securely mounted onto a Synthia MK II laboratory system. The time and power control were located outside a lead-shielded hot-cell and linked to the cavity through an RF coaxial cable. The reaction V-vial (1 mL volume, Alltech Associates, Deerfield, IL) was equipped with a screw-on cap and septum (Tuf-Bond Teflon/silicone; Pierce Biotechnology Inc., Rockford, IL). The septum was pierced with a vent needle that was connected to a glass vial (20 mL) in order to collect evaporated solvents and also to a charcoal trap to retain any break-through of volatile radioactive species. Liquid handling was achieved with a Gilson Aspec autoinjector/dispenser, which forms part of the Synthia apparatus. Other operations of the radiosynthesis and purification procedures were controlled by a Visual Chemistry-based recipe. Heating time and power input were controlled independently.

[^{18}F]Fluoride ion (∼300 mCi) in ^{18}O-enriched water (350−500 μL) was dried in the V-vial containing K 2.2.2 (5 mg), K_2CO_3 (0.5 mg) in acetonitrile/water (9:1 v/v, 100 μL). Microwave heating (90 W in 3 pulses of 2 min, 130 °C) was applied under N_2 gas flow (200 mL/min) to speed up the removal of the azeotropic water−acetonitrile mixture. The heating cycle was repeated twice, and each time fresh acetonitrile (500 μL) was added. Precursor **8** (∼0.85 ± 0.1 mg) in acetonitrile (to reach a concentration of 1 mg/mL) was introduced into the V-vial and heated at 70 °C (15−35 W in two pulses, each of 1 min). After cooling, the reaction mixture was diluted with mobile phase (0.75 mL) and injected onto a Luna C18 column (3 μm, 250 mm × 10 mm; Phenomenex) eluted at 3 mL/min with a mixture of A (water) and B (acetonitrile) according to the program: 30% B for 3 min, then 47% B over 4 min and holding to 47% B over 80 min ([^{18}F]**9**, t_R = 78 min). Formulation of [^{18}F]**9** was performed as described above.

The radiochemical purity and specific radioactivity of the formulated [^{18}F]**9** were calculated by injecting a sample of the radioactive solution (0.2−0.5 mCi) into a Luna hexyl phenyl column (3 μm, 150 mm × 4.6 mm; Phenomenex) eluted with MeCN-10 mM ammonium formate (60:40 v/v) at 1 mL/min ([^{18}F]**9**, t_R = 6.7 min). The absorbance response (at 230 nm) was calibrated with respect to mass of **9**.

Computation of cLogP and cLogD, and Measurement of LogD. cLogP and cLogD (at pH = 7.4) values for **1** and **9** were computed with the program Pallas 3.0 for Windows (CompuDrug; S. San Francisco, CA).

The LogD value of [^{18}F]**9** was measured as the log of its distribution coefficient between *n*-octanol and sodium phosphate buffer (0.15 M, pH 7.4), as described previously in detail for other radioligands.[26]

PET Experiments with [^{18}F]9 in Monkeys. Three male rhesus (*Mucacca mulatto*) monkeys (11−15 kg) were scanned at baseline for up to 300 min to measure uptake of radioactivity into brain and to determine activity distribution after bolus intravenous injection of [^{18}F]**9** (2.76−5.80 mCi; dose of **9**, 0.068−0.276 μg/kg). A preblock experiment was also performed in one of the monkeys (14 kg) in which **1** (3 mg/kg, iv) was administered at 24 min before [^{18}F]**9** (5.09 mCi; 0.323 μg/kg of **9**) and the monkey imaged for 120 min from radioligand injection. One of the monkeys (15 kg) was also scanned for 240 min from the intravenous injection of a bolus of [^{18}F]**9** (1.28 mCi; dose of **9**, 0.12 μg/kg) with **1** (3 mg/kg, iv) administered at 60 min from the start of the scan.

For each scanning session, the monkey subject was immobilized with ketamine and maintained under anesthesia with 1.6% isoflurane in oxygen. An intravenous perfusion line filled with saline (0.9% w/v) was used for bolus injection of [^{18}F]**9**. PET serial dynamic images were obtained on an Advance (GE Medical Systems WI) or High Resolution Research Tomograph (Siemens/CPS, Knoxville, TN) PET camera. Decay-corrected time-activity curves (TACs) were obtained for irregular volumes of interest (VOIs), selected from frontal cortex, temporal cortex, parietal cortex, occipital cortex, striatum, thalamus, cerebellum, and to choroid plexus on fourth ventricle. Radioactivity was normalized for injected dose and monkey weight by expression as % standardized uptake value [%SUV = (% injected dose per g) × body weight in g].

MRI and Image Fusion. All monkeys had T1-weighted magnetic resonance imaging (TR/TE/x = 24 ms/3 ms/300), acquired on a 1.5-T Horizon instrument (GE Medical Systems, Waukesha, WI). PET and MR images were coregistered with SPM2 software (Wellcome Department of Cognitive Neurology, London, UK).

Stability of [^{18}F]9 in Monkey Whole Blood and Plasma in Vitro, and in Buffer. [^{18}F]**9** was incubated for 45 min in whole monkey blood (1 mL). A sample (0.5 mL) was removed, added to acetonitrile (0.8 mL), and centrifuged. Then the supernatant liquid was analyzed by reverse phase radio-HPLC (see General Methods). The stability of [^{18}F]**9** to incubation in sodium phosphate buffer (0.15 M, pH 7.4) for 2 h at room temperature was also assessed by HPLC.

Plasma Protein Binding of [^{18}F]9.[59] The radioligand was added to pooled human plasma, placed at the top of an "Amicon" Centrifree filter unit (200 μL/unit) and filtered by ultra centrifugation at 5000*g*. Then all components of filter units were counted for radioactivity. The distribution of [^{18}F]**9** between the plasma and the cellular component of the blood was determined in vitro by incubating [^{18}F]**9** with monkey whole blood, centrifugation, and measuring radioactivity associated with plasma and cells.

Emergence of Radiometabolites of [^{18}F]9 in Monkey Plasma In Vivo. During each of four PET scans (three baseline and one preblock), blood samples were drawn periodically from the monkey femoral artery and collected in heparin-treated Vacutainer tubes. The samples were centrifuged and the plasma separated. A sample of plasma (1 mL) was mixed with acetonitrile (1.5 mL) and centrifuged. The supernatant liquid was analyzed with radio-HPLC (see General Methods). The percentages of [^{18}F]**9** and its radiometabolites were calculated.

Stability of [^{18}F]9 to Rat Brain In Vitro. Brains from two rats were excised. The brain (1.44 g) from one rat was homogenized in saline (1 mL) plus acetonitrile (2 mL), doped with [^{18}F]**9** (2 μCi), rehomogenized, and centrifuged. The other brain (1.70 g) was homogenized in saline (3 mL), doped with [^{18}F]**9** (5 μCi), and incubated at 37 °C. Samples (200 μL; n = 6) were removed from the incubate periodically up to 60 min, placed in acetonitrile (700 μL), and centrifuged. Each supernatant liquid was analyzed with radio-HPLC. The percentages of radioactivity represented by [^{18}F]**9** and its radiometabolites were calculated.

Emergence of Radiometabolites of [^{18}F]9 in Rat Plasma, Urine and Brain In Vivo. Four rats (277−623 g) were anesthetized by inhalation of 1.5% isoflurane in oxygen and maintained at 37 °C with a heating pad. Two of the rats were each injected with a bolus of formulated NCA [^{18}F]**9** (0.812 or 1.32 mCi; specific radioactivity >1.39 Ci/μmol), and the other two with a bolus of CA [^{18}F]**9** (0.86 or 0.89 mCi) of known specific radioactivity (~0.13 Ci/μmol). The CA doses were formulated in saline (2.0 mL) containing ethanol (10% v/v) and Tween 80 (5% w/v) In the CA experiment, expression of urine was assured by ip administration of saline (5 mL) at 30 min before [^{18}F]**9**. Blood samples were drawn from each rat at intervals for radio-HPLC analysis of harvested and deproteinized plasma. Each rat was then sacrificed at a set time after injection (30 and 95 min for the two rats administered NCA [^{18}F]**9** and 60 min for those administered CA [^{18}F]**9**). Urine was collected at 60 min for radio-HPLC analysis from the two rats administered CA [^{18}F]**9**. The brain from each rat was excised, homogenized in an ice-bath in saline (1 mL) plus acetonitrile (2 mL), further homogenized after addition of water (0.5 mL), and finally centrifuged. The supernatant liquids were analyzed with radio-HPLC. The percentages of radioactivity represented by [^{18}F]**9** and its radiometabolites were calculated for each brain, urine, and plasma analyte.

LC-MS-MS Search for Metabolites of 3 Emerging in Rat Brain, Urine and Plasma in Vivo. Three healthy rats (480 ± 203) were placed under isoflurane (1.5% in oxygen) anesthesia and injected through the penile vein over 9 min with compound **9** (2.26 ± 0.76 mg) in saline (0.9 mL) containing ethanol (10% v/v) and either Cremophor EL (30 mg) or Tween 80 (30 mg). The urethras were clamped and every 30 min the rats were intravenously administered with saline (0.1 mL). After 60 or 115 min, blood and urine samples (1.0−2.0 mL) were collected and the rats were sacrificed by injection of saturated KCl solution or increased anesthesia. The brains were immediately excised and each homogenized in acetonitrile (3.0 mL) with a "Tissue Tearor". Water (500 μL) was added and the tissue rehomogenized before centrifugation at 10000*g* for 10 min. The clear supernatant liquid was collected and the precipitate rehomogenized and centrifuged as before. The supernatant liquid was added to that previously collected and stored at − 70 °C preceding LC-MS-MS analysis (see General Methods). Urine samples were stored and analyzed in the same way. Collected blood samples were stored similarly and, preceding analysis, plasma was harvested and deproteinized with acetonitrile.

Emergence of Radiometabolites of [^{18}F]11 in Rat Brain and Plasma In Vitro. Two rats (497 and 449 g) were anesthetized with 1.5% isoflurane in oxygen. Whole blood was drawn from each rat by cardiac puncture and then the rat sacrificed by excess anesthesia. The brain of one rat was excised and placed on ice without perfusion. The brain of the second rat was perfused with heparinized ice-cold saline until perfusate ran clear and then placed on ice. Each brain was separately homogenized in saline (3 mL) while on ice. [^{18}F]**11** (~10 μCi) in formulation vehicle (100 μL) was then added to each brain homogenate, which was then incubated at 37 °C for 60 min and then analyzed by radio-HPLC.

Emergence of Radiometabolites of [^{18}F]11 in Rat Brain and Plasma Ex Vivo. One rat (429 g) was anesthetized with 1.5% isoflurane in oxygen and then maintained at 37 °C with a heating pad. The rat was injected with [^{18}F]**11** (74.6 μCi) in formulation vehicle (1 mL) through the penile vein over 4 min. After 30 min, blood was withdrawn via cardiac puncture into a heparinized syringe. The brain was excised, measured for radioactivity in a

γ-counter, and then homogenized in acetonitrile (2 mL) with a Tissue Tearor. Water (0.5 mL) was added and the tissue rehomogenized, measured for radioactivity, and centrifuged at 10000*g* for 1 min. The clear supernatant liquid was analyzed by radio-HPLC and the precipitate measured for radioactivity. A whole blood sample and an aliquot of its plasma were also measured.

Evaluation of the Rat Brain Penetration of the Radiometabolite(s) of [^{18}F]11. [^{18}F]**11** (87 μCi) in formulation vehicle (1.7 mL) was incubated with anticoagulated blood (4.0 mL) for 30 min. An aliquot of the blood was then removed and the plasma harvested and deproteinized with acetonitrile. Analysis of the plasma by radio-HPLC showed that the radioactivity was 99.9% polar radiometabolite(s). Radioactive plasma was then harvested from the remaining whole blood (~4.0 mL) and administered to another anesthetized rat. After 30 min, anticoagulated blood was drawn and the rat sacrificed. The radioactivities (%SUV) in blood and in harvested plasma were measured. The brain was excised and measured for radioactivity (%SUV).

Acknowledgment. This study was supported by the Intramural Research Program of the National Institutes of Health, specifically the National Institute of Mental Health (project no. Z01-MH-002793). We thank Kimberley Jenko for assistance on experiments in rats. We also thank the NIH PET Department for fluorine-18 production and successful completion of the scanning experiments, and PMOD Technologies for providing the image analysis software.

Supporting Information Available: HPLC chromatograms verifying the purities of compounds **8**−**11**. This material is available free of charge via the Internet at http://pubs.acs.org.

References

(1) McEnery, M. W.; Snowman, A. M.; Trifletti, R. R.; Snyder, S. H. Isolation of the mitochondrial benzodiazepine receptor: association with the voltage dependent anion channel and the adenine nucleotide carrier. *Proc. Natl. Acad. Sci. U.S.A.* **1992**, *89*, 3170–3174.
(2) Schoemaker, H.; Bliss, M.; Yamamura, H. I. Specific high-affinity saturable binding of [^{3}H]Ro5-4864 to benzodiazepine binding sites in the rat cerebral cortex. *Eur. J. Pharmacol.* **1981**, *71*, 173–175.
(3) Braestrup, C.; Albrechtsen, R.; Squires, R. F. High densities of benzodiazepine receptors in human cortical areas. *Nature* **1977**, *269*, 702–704.
(4) Anholt, R. R.; De Souza, E. B.; Oster-Granite, M. L.; Snyder, S. H. Peripheral-type benzodiazepine receptors: autoradiographic localization in whole body sections of neonatal rats. *J. Pharmacol. Exp. Ther.* **1985**, *233*, 517–526.
(5) Parola, A. L.; Yamamura, H. I.; Laird II, H. E. Peripheral-type benzodiazepine receptors. *Life Sci.* **1993**, *52*, 1329–1342.
(6) Papadopoulos, V.; Baraldi, M.; Guilarte, T. R.; Knudsen, T. B.; Lacapère, J. J.; Lindemann, P.; Norenberg, M. D.; Nutt, D.; Weizman, A.; Zhang, M. R.; Gavish, M. Translocator protein (18 kDa): new nomenclature for the peripheral-type benzodiazepine receptor based on its structure and molecular function. *Trends Pharmacol. Sci.* **2006**, *27*, 402–409.
(7) Lacapère, J.-J.; Papadopoulos, V. Peripheral-type benzodiazepine receptor: structure and function of a cholesterol-binding protein in steroid and bile acid synthesis. *Steroids* **2003**, *68*, 569–585.
(8) Papadopoulos, V.; Amri, H.; Li, H.; Boujrad, N.; Vidic, B.; Garnier, M. Target disruption of the peripheral-type benzodiazepine receptor gene inhibits steroidogenesis in the R2C Leydig tumor cell line. *J. Biol. Chem.* **1997**, *272*, 32129–32135.
(9) Taketani, S.; Kohno, H.; Furukawa, T.; Tokunaga, R. Involvement of peripheral-type benzodiazepine receptors in the intracellular-transport of heme and porphyrins. *J. Biochem.* **1995**, *117*, 875–880.
(10) Zavala, F. Benzodiazepines, anxiety and immunity. *Pharmacol. Ther.* **1997**, *75*, 199–216.
(11) Verma, A.; Facchina, S. L.; Hirsch, D. J.; Song, S. Y.; Dillahey, L. F.; Williams, J. R.; Snyder, S. H. Photodynamic tumor therapy: mitochondrial benzodiazepeine receptors as a therapeutic target. *Mol. Med.* **1998**, *4*, 40–45.
(12) Chelli, B.; Lena, A.; Vanacore, R.; Pozzo, E. D.; Costa, B.; Salvetti, A.; Scatena, F.; Ceruti, S.; Abbracchio, M. P.; Gremigni, V.; Martini, C. Peripheral benzodiazepine receptor ligands: mitochondrial transmembrane potential depolarization and apoptosis induction in rat C6 glioma cells. *Biochem. Pharmacol.* **2004**, *68*, 125–134.
(13) Myers, R.; Manjil, L. G.; Cullen, B. M.; Price, G. W.; Frackowiak, R. S.; Cremer, J. E. Macrophage and astrocyte populations in relation to [^{3}H]PK 11195 binding in rat cerebral cortex following a local ischemic lesion. *J. Cereb. Blood Flow Metab.* **1991**, *11*, 314–322.
(14) Syapin, P. J.; Skolnick, P. Characterization of benzodiazepine binding sites in cultured cells of neural origin. *J. Neurochem.* **1979**, *32*, 1047–1051.
(15) Lang, S. The role of peripheral benzodiazepine receptors (PBRs) in CNS pathophysiology. *Curr. Med. Chem.* **2002**, *9*, 1411–1415.
(16) Papadopoulos, V.; Lecanu, L.; Brown, R. C.; Han, Z.; Yao, Z. X. Peripheral-type benzodiazepine receptor in neurosteroid biosynthesis, neuropathology and neurological disorders. *Neurosci.* **2006**, *138*, 749–756.
(17) Benavides, J.; Fage, D.; Carter, C.; Scatton, B. Peripheral type benzodiazepine binding sites are a sensitive indirect index of neuronal damage. *Brain Res.* **1987**, *421*, 167–172.
(18) Wilms, H.; Claasen, J.; Röhl, C.; Siervers, J.; Deuschl, G.; Lucius, R. Involvement of benzodiazepine receptors in neuroinflammatory and neurodegenerative diseases: evidence from activated microglial cells in vitro. *Neurobiol. Dis.* **2003**, *14*, 417–424.
(19) Camsonne, R.; Crouzel, C.; Comar, D.; Mazière, M.; Prenant, C.; Sastre, J.; Moulin, M. A.; Syrota, A. Synthesis of 1-(2-chlorophenyl)-*N*-[^{11}C]methyl-*N*-(1-methylpropyl)-3-isoquinoline carboxamide (PK 11195): a new ligand for peripheral benzodiazepine receptors. *J. Labelled Compd. Radiopharm.* **1984**, *21*, 985–991.
(20) Shah, F.; Hume, S. P.; Pike, V. W.; Ashworth, S.; McDermott, J. Synthesis of the enantiomers of [*N*-methyl-^{11}C]PK 11195 and comparison of their behaviours as radioligands for PK binding sites in rats. *Nucl. Med. Biol.* **1994**, *21*, 573–581.
(21) Cagnin, A.; Kassiou, M.; Meikle, S. R.; Banati, R. B. Positron emission tomography imaging of neuroinflammation. *Neurotherapeutics* **2007**, *4*, 443–452.
(22) Venneti, S.; Lopresti, B. J.; Wiley, A. A. The peripheral benzodiazepine receptor (translocator protein 18 kDA) in microglia: from pathology to imaging. *Prog. Neurobiol.* **2006**, *80*, 308–322.
(23) James, M. L.; Selleri, S.; Kassiou, M. Development of ligands for the peripheral benzodiazepine receptor. *Curr. Med. Chem.* **2006**, *13*, 1991–2001.
(24) Okuyama, S.; Chaki, S.; Yoshikawa, R.; Ogawa, S.; Suzuki, Y.; Okubo, T.; Nakazato, A.; Nagamine, M.; Tomisawa, K. Neuropharmacological profile of peripheral benzodiazepine receptor agonists, DAA 1097 and DAA 1106. *Life Sci.* **1999**, *64*, 1455–1464.
(25) Zhang, M.-R.; Kida, T.; Noguchi, J.; Furuitsuka, K.; Maeda, J.; Suhara, T.; Suzuki, K. [^{11}C]DAA1106: radiosynthesis and in vivo binding to peripheral benzodiazepine receptors in mouse brain. *Nucl. Med. Biol.* **2003**, *30*, 513–519.
(26) Briard, E.; Zoghbi, S. S.; Imaizumi, M.; Gourley, J. P.; Hong, J.; Cropley, V.; Fujita, M.; Innis, R. B.; Pike, V. W. Synthesis and evaluation in monkey of two sensitive ^{11}C-labeled aryloxyanilide ligands for imaging brain peripheral benzodiazepine receptors in vivo. *J. Med. Chem.* **2008**, *51*, 17–30.
(27) Brown, A. K.; Fujita, M.; Fujimura, Y.; Liow, J.-S.; Stabin, M.; Ryu, Y. H.; Imaizumi, M.; Hong, J.; Pike, V. W.; Innis, R. B. Radiation dosimetry and biodistribution in monkey and man of 11C-PBR28, a PET radioligand to image inflammation. *J. Nucl. Med.* **2007**, *48*, 2072–2079.
(28) Imaizumi, M.; Briard, E.; Zoghbi, S. S.; Gourley, J. P.; Hong, J.; Fujimura, Y.; Pike, V. W.; Innis, R. B.; Fujita, M. Brain and whole-body imaging in nonhuman primates of [^{11}C]PBR28, a promising radioligand for peripheral benzodiazepine receptors. *NeuroImage* **2008**, *39*, 1289–1298.
(29) Fujita, M.; Imaizumi, M.; Zoghbi, S. S.; Fujimura, Y.; Farris, A. G.; Suhara, T.; Hong, J.; Pike, V. W.; Innis, R. B. Kinetic analysis in healthy humans of a novel positron emission tomography radioligand to image the peripheral benzodiazepine receptor, a potential biomarker for inflammation. *NeuroImage* **2008**, *40*, 43–52.
(30) Guillaume, M.; Luxen, A.; Nebeling, R.; Argentini, M.; Clark, J. C.; Pike, V. W. Recommendations for fluorine-18 production. *Appl. Radiat. Isot.* **1991**, *42*, 749–762.
(31) Zhang, M. R.; Maeda, J.; Furutsuka, K.; Yoshida, Y.; Ogawa, M.; Suhara, T.; Suzuki, K. [^{18}F]FMDAA1106 and [^{18}F]FEDAA1106: two positron-emitter labeled ligands for peripheral benzodiazepine receptor (PBR). *Bioorg. Med. Chem. Lett.* **2003**, *13*, 201–204.
(32) Zhang, M.-R.; Maeda, J.; Ogawa, M.; Noguchi, J.; Ito, J.; Yoshida, Y.; Okauchi, T.; Obayashi, S.; Suhara, T.; Suzuki, K. Development of a new radioligand, *N*-(5-fluoro-2-phenoxyphenyl)-*N*-(2-[^{18}F]fluoroethyl-5-methoxybenzyl)acetamide, for PET imaging of peripheral benzodiazepine receptor in primate brain. *J. Med. Chem.* **2004**, *47*, 2228–2235.
(33) Fujimura, Y.; Ikoma, Y.; Yasuno, F.; Suhara, T.; Ota, M.; Matsumoto, R.; Nozaki, S.; Takano, A.; Kosaka, J.; Zhang, M.-R.; Nakao, R.; Suzuki, K.; Kato, N.; Ito, H. Quantitative analyses of ^{18}F-FEDAA1106

binding to peripheral benzodiazepine receptors in living human brain. *J. Nucl. Med.* **2006**, *47*, 43–50.
(34) Zhang, M.-R.; Kumata, K.; Suzuki, K. A practical route for synthesizing a PET ligand containing [^{18}F]fluorobenzene using reaction of diphenyliodonium salt with [^{18}F]F$^-$. *Tetrahedron Lett.* **2007**, *48*, 8632–8635.
(35) Maeda, J.; Suhara, T.; Zhang, M. R.; Okauchi, T.; Yasuno, F.; Ikoma, Y.; Inaji, M.; Nagai, Y.; Takano, A.; Obayashi, S.; Suzuki, K. Novel peripheral benzodiazepine receptor ligand [^{11}C]DAA1106 for PET: an imaging tool for glial cells in brain. *Synapse* **2004**, *52*, 283–291.
(36) Wilson, A. A.; Garcia, A.; Parkes, J.; McCormick, P.; Stephenson, K. A.; Houle, S.; Vasdev, N. Radiosynthesis and initial evaluation of [^{18}F]-FEPPA for PET imaging of peripheral benzodiazepine receptors. *Nucl. Med. Biol.* **2008**, *35*, 305–314.
(37) Pascali, C.; Luthra, S. K.; Pike, V. W.; Price, G. W.; Ahier, R. G.; Hume, S. P.; Myers, R.; Manjil, L.; Cremer, J. E. The radiosynthesis of [^{18}F]PK 14105 as an alternative radioligand for peripheral type benzodiazepine binding sites. *Appl. Radiat. Isot.* **1990**, *41*, 477–482.
(38) Price, G. W.; Ahier, R. G.; Hume, S. P.; Myers, R.; Manjil, L.; Cremer, J. E.; Luthra, S. K.; Pascali, C.; Pike, V. W.; Frackowiak, R. In vivo binding to peripheral benzodiazepine binding sites in lesioned rat brain: comparison between [^{3}H]PK 11195 and [^{18}F]PK 14105 as markers for neuronal damage. *J. Neurochem.* **1990**, *55*, 175–185.
(39) Yu, W.; Wang, E.; Voll, R. J.; Miller, A. H.; Goodman, M. M. Synthesis, fluorine-18 radiolabeling and in vitro characterization of 1-iodophenyl-*N*-methyl-*N*-fluoroalkyl-3-isoquinoline carboxamide derivatives as potential PET radioligands for imaging peripheral benzodiazepine receptors. *Bioorg. Med. Chem.* **2008**, *16*, 6145–6155.
(40) Fookes, C. J. R.; Pham, T. Q.; Mattner, F.; Greguric, I.; Loc'h, C.; Liu, X.; Berghofer, P.; Shephard, R.; Gregoire, M.-C.; Katsifis, A. Synthesis and biological evaluation of substituted [^{18}F]imidazo[1,2-*a*]pyridines and [^{18}F]pyrazolo[1,5-*a*]pyrimidines for the study of the peripheral benzodiazepine receptor using positron emission tomography. *J. Med. Chem.* **2008**, *51*, 3700–3712.
(41) Bjurling, P.; Reineck, R.; Westerberg, G.; Gee, A. D.; Sutcliffe, J.; Långström, B. *Proc. VIth Workshop on Targetry and Target Chemistry*, TRIUMF, Vancouver, Canada, 1995, pp. 282−284.
(42) Lazarova, N.; Siméon, F. G.; Musachio, J. L.; Lu, S.; Pike, V. W. Integration of a microwave reactor with Synthia to provide a fully automated radiofluorination module. *J. Labelled Compd. Radiopharm.* **2007**, *50*, 463–465.
(43) Pike, V. W. Positron-emitting radioligands for studies in vivo—probes for human psychopharmacology. *J. Psychopharmacol.* **1993**, *7*, 139–158.
(44) Laruelle, M.; Slifstein, M.; Huang, Y. Relationships between radiotracer properties and image quality in molecular imaging of the brain with positron emission tomography. *Mol. Imaging Biol.* **2003**, *5*, 363–375.
(45) Okubo, T.; Yoshikawa, R.; Chaki, S.; Okuyama, S.; Nakazato, A. Design, synthesis and structure−affinity relationships of aryloxyanilide derivatives as novel peripheral benzodiazepine receptor ligands. *Bioorg. Med. Chem.* **2004**, *12*, 423–438.
(46) Nakazato, A.; Okubo, T.; Nakamura, T.; Chagi, S.; Tomisawa, K.; Nagamine, M.; Yamamoto, K.; Harade, K.; Yoshida, M. Aryloxy nitrogen-containing heteroarylamines derivative, their use and MDR ligands containing them. JP Patent 001476, 2000. in Japanese.
(47) Nakazato, A.; Okubo, T.; Nakamura, T.; Shigeyuki, C.; Kazuyuki, T.; Nagamine, M.; Yamamoto, K.; Harada, K.; Yoshida, M. Heterocycle substituted aryloxyaniline derivatives and their uses as MDR ligands. U.S. Patent 6,476,056 B2, 2002.
(48) Briard, E.; Pike, V. W. Substitution-reduction−an alternative process for the no-carrier-added [^{18}F]*N*-(2-fluoroethylation) of anilines. *J. Labelled Compd. Radiopharm.* **2004**, *47*, 217–232.
(49) Waterhouse, R. N. Determination of lipophilicity and its use as a predictor of blood−brain barrier penetration of molecular imaging agents. *Mol. Imaging Biol.* **2003**, *5*, 376–389.
(50) Imaizumi, M.; Briard, E.; Zoghbi, S. S.; Gourley, J. P.; Hong, J.; Musachio, J. L.; Gladding, R.; Pike, V. W.; Innis, R. B.; Fujita, M. Kinetic evaluation in nonhuman primates of two new PET ligands for peripheral benzodiazepine receptors in brain. *Synapse* **2007**, *61*, 595–605.
(51) Cai, L.; Lu, S. Y.; Pike, V. W. Chemistry with [^{18}F]fluoride ion. *Eur. J. Org. Chem.* **2008**, *17*, 2853–2873.
(52) Canat, X.; Caryon, P.; Bouaboula, M.; Cahard, D.; Shire, D.; Roque, C.; Le Fur, G.; Casellas, P. Distribution profile and properties of peripheral-type benzodiazepine receptors on human hemopoietic cells. *Life Sci.* **1992**, *52*, 107–118.
(53) Olson, J. M. M.; Ciliax, B. J.; Mancini, W. R.; Young, A. B. Presence of peripheral type benzodiazepine binding sites on human erythrocyte membranes. *Eur. J. Pharmacol.* **1988**, *152*, 47–53.
(54) Cymerman, U.; Pazos, A.; Palacios, J. M. Evidence for species differences in "peripheral" benzodiazepine receptors: an autoradiographic study. *Neurosci. Lett.* **1986**, *66*, 153–158.
(55) Ponder, D. E.; Dence, C. S.; Oyama, N.; Kim, J.; Tai, Y. C.; Laforest, R.; Siegel, B. A.; Welch, M. J. [^{18}F]Fluoroacetate a potential analog for prostate tumor imaging—in vivo evaluation of [^{18}F]fluoroacetate versus [^{11}C]acetate. *J. Nucl. Med.* **2007**, *48*, 420–428.
(56) Sykes, T. R.; Ruth, T. J.; Adam, M. J. Synthesis and murine uptake of sodium [^{18}F]fluoroacetate. *Nucl. Med. Biol.* **1986**, *13*, 497–500.
(57) Clark, J. D.; Baldwin, R. L.; Bayne, K. A.; Brown, M. J.; Gebhart, G. F.; Gonder, J. C.; Gwathmey, J. K.; Keeling, M. E.; Kohn, D. F.; Robb, J. W.; Smith, O. A.; Steggerda, J.-A. D.; VandeBer, J. L. *Guide for the Care and Use of Laboratory Animals*; National Academy Press: Washington DC, 1996.
(58) Chaki, S.; Funakoshi, T.; Yoshikawa, R.; Okuyama, S.; Okubo, T.; Nakazato, A.; Nagamine, M.; Tomisawa, K. Binding characteristics of [^{3}H]DAA1106, a novel and selective ligand for peripheral benzodiazepine receptors. *Eur. J. Pharmacol.* **1999**, *371*, 197–204.
(59) Gandelman, M. S.; Baldwin, R. M.; Zoghbi, S. S.; Zea-Ponce, Y.; Innis, R. B. Evaluation of ultrafiltration for the free-fraction determination of single photon emission computed tomography (SPECT) radiotracers: β-CIT, IBF, and iomazenil. *J. Pharm. Sci.* **1994**, *83*, 1014–1019.

JM8011855